Elastic and Anelastic Structure Beneath Eurasia

Göran Ekström, Adam M. Dziewonski, Wei-jia Su and Gideon P. Smith

Department of Earth and Planetary Sciences
Harvard University
Cambridge, MA 02138

Abstract

We are collecting and analyzing large and diverse datasets of seismic waveforms, absolute and relative body wave traveltimes, and surface wave phase velocities and amplitudes. Our primary objective is to map the variations of elastic mantle properties beneath Eurasia over horizontal lengthscales of approximately 1000–1500 km and vertical lengthscales of 50–100 km. In comparison with recent Harvard global models, such as S12WM13, we have increased the horizontal resolution by expanding the global structure up to spherical harmonic degree $l = 20$, and we have adopted a radial parameterization which gives better vertical resolution in the upper mantle.

Using earlier and new datasets, we have derived a new whole mantle model, S20U7L5. The new model shows many of the same features seen in previous tomographic images, but with significantly sharper definition, in particular in the upper mantle. Lithospheric roots beneath the stable continental interiors are the most prominent feature in the uppermost mantle. The model is partially validated by comparisons with the earlier regional models SNA and TNA. While there is striking similarity in the velocity structure beneath a great variety of continental interiors, West Africa appears to overlie one of the fastest locations in the upper mantle, with faster than average velocities extending to 500 km depth.

Additional tasks to be completed before the new model is finalized is the incorporation of more accurate corrections for crustal thickness and structure, as well as the inclusion of an extensive dataset of recently measured teleseismic traveltimes.

Objective

We are adapting the seismic tomographic techniques developed in global scale studies to the regional scale problem of mapping the elastic and anelastic material properties beneath Eurasia. The main objective of this research is to obtain a tomographic seismic velocity model for the structure beneath Eurasia with a horizontal resolution corresponding to at least $l = 20$, consistent with the widest possible range of seismological observations. Related objectives are to evaluate the resulting model and its utility in event location algorithms.

Research Accomplished

In earlier reports (1993, 1994) we have presented results based on earlier whole mantle and preliminary upper mantle models, while also addressing the question of teleseismic event locations using heterogeneous mantle models. In this report we describe in greater detail the derivation of the new global mantle model S20U7L5. We discuss and compare some shallow mantel structures seen in this model with previously derived regional models, and point out some remaining problems/issues which we plan to address before producing the final version of the model.

A degree 20 model of the Mantle

Earlier tomographic models of the whole mantle, based on a variety of datasets, have provided descriptions of large, planetary-scale variations of P and S velocities in the mantle. With the goal of obtaining better resolution of structures, particularly for the upper mantle, we have collected and incorporated high-quality surface wave dispersion data with the previously developed, and now expanded, seismological datasets of travel times and body and mantle wave waveforms in the model inversion. The new model is parameterized to preferentially resolve smaller-scale structures in the upper mantle, while at the same time accounting for the dominantly large-scale structures in the lower mantle.

Parameterization

The parameterization and inversion approach are similar to those used for earlier Harvard mantle models, such as S12WM13 (Su *et al.*, 1993), with the following notable differences:

- We use a split parameterization for the mantle, and parameterize the radial variations in the upper mantle in terms of Chebyshev polynomials of degree 0–7. For the lower mantle we use Chebyshev polynomials of degree 0–5. This split parameterization, with more degrees of freedom in the upper mantle, reflects our goal of resolving primarily the shallow mantle structure, and the greater sensitivity of our data sets to heterogeneity in the upper mantle (see below).

- The spherical harmonic expansion is extended from degree 12 to degree 20. If we assume that we can resolve structures of dimensions that are approximately half the minimum wavelength of the highest harmonic, this implies a resolving length of $\sim$1000 km. The new parameterization increases the number of parameters to be determined for each radial degree from 169 to 441, and the total number of unknown coefficients is $14 \times 441 = 6174$. While we do not expect to be able to resolve degree 20 structure in the deeper mantle, due to our data coverage, we do believe that this resolution is

achievable in the top several hundred kilometers of the upper mantle. We damp the spatial derivatives of the model in the inversions, and a higher damping is applied to the lower mantle.

- The data are corrected for crustal structure using a new compilation of crustal thicknesses by Mooney (1994). This is in contrast to previous models which were only corrected for average continental and oceanic crustal structure. The crustal correction is important for explaining phase velocities of shorter period surface waves.

Data Sources

Several types of data with sensitivity to velocity variations in different parts of the mantle are included. So far, the following data have been incorporated in the derivation of the new model, which we call S20U7L5 (spherical harmonic degree 20, degree 7 in the upper mantle and degree 5 in the lower mantle):

- Absolute and differential travel times measured from waveform data (S, SS, ScS, $SS - S$). These are the same data sets that were used in the development of S12WM13.

- Long-period body and mantle waveforms from 451 earthquakes recorded on the Global Seismic Network. This dataset is similar in coverage to the data that were used for S12WM13, but we use a more broadband spectral weighting in the waveform fitting.

- Dispersion measurements of Rayleigh waves at 140, 100, and 75 seconds (described below).

- Dispersion measurements of Love waves at 140, 100, 75, 60, and 50 seconds (described below).

The Love wave and Rayleigh wave dispersion datasets have not previously been used in inversions for mantle structure, and they are described in some detail in the next section.

Dispersion of Love and Rayleigh waves

The method developed by Ekström *et al.* (1993) matches an observed surface waves seismogram $o(t)$ with a model seismograms $m(t)$ through iterative adjustment of parameters which describe the dispersion and amplitude spectrum of the model waveform. A fundamental mode model waveform $m(t)$ is calculated using the JWKB expressions for surface waves, which reduce to

$$m(\omega) = A(\omega) \exp[i\Phi(\omega)]. \tag{1}$$

The propagation part of the phase is expressed as

$$\Phi_P(\omega) = \frac{\omega X}{c^\circ(\omega) + \delta c(\omega)} \tag{2}$$

where $\delta c(\omega)$ is the average phase velocity perturbation with respect to the PREM value c°. The amplitude function $A(\omega)$ and the phase velocity perturbation $\delta c(\omega)$ are parameterized as smooth B-spline functions of the period band of interest, 35–150 seconds. Since the adjustment of $m(t)$ to resemble $o(t)$ cannot be determined by direct linear inversion, an

iterative, non-linear algorithm was developed. The algorithm is based on two concepts: *Iterative Frequency Band Expansion*, and *Iterative Phase Isolation and Minimization of Residual Dispersion*, which are integrated in the following algorithm:

1. Spline parameters for surface wave dispersion and amplitudes are calculated for an initial Earth model, for example S12WM13, and a trial model seismogram is calculated.

2. Observed and model seismograms are filtered between 75–125 sec, the initial frequency window.

3. Dispersion and amplitudes are adjusted to maximize the fit in the current frequency window.

   - Observed and model seismograms are cross correlated, and the model seismogram is auto correlated.
   - An objective function is formed which reflects the difference between the cross- and autocorrelations.
   - Spline coefficients for $\delta c(\omega)$ and $A(\omega)$ are iteratively adjusted to minimize the objective function.

4. The frequency window is expanded to higher and lower frequencies.

5. Steps 3 and 4 are repeated until the whole frequency band of interest is included.

Ekström *et al.* (1993) automated this algorithm and applied it systematically to surface waves recorded on GSN, CDSN, GEOSCOPE, and MedNet stations. Moderate and large earthquakes over a 4-year-period have now been used, and more than 80,000 paths were analyzed, out of which approximately 10,000 Rayleigh and 8,000 Love waves were of high quality. Ekström *et al.* have reported on the derivation from these data of phase velocity maps, but in the derivation of S20U7L5, the raw phase anomalies were used and treated in the same way as travel times.

Inversion Results

The new model S20U7L5 shows many of the same features seen in previous tomographic images, but with significantly sharper definition. Figure 1 shows a comparison between the S velocity perturbations at 150 km depth beneath the Mediterranean and North Africa as imaged in S12WM13 (top) and in the new model S20U7L5 (bottom). Many features, such as the very fast West African craton and the slow velocities coincident with the Cameroon line are much clearer in the new model. The slow velocities associated with the Red Sea rift are also much better defined in S20U7L5. While the new model shows much greater lateral contrasts in the upper mantle, the low angular degree components of the new model in general agree very well with previous mantle models such as S12WM13.

On a global scale, the fast velocities beneath stable continental interiors is the most prominent anomaly in the top 300 km of the mantle. The very high velocities beneath the stable interior of West Africa continue even deeper, as can be seen in a velocity profile (Figure 2). The new model also shows that the slow velocity anomalies associated with ridges continue to great depth, in particular in the Indian Ocean. The Red Sea rift shows slow velocities

extending down to 400 km (Figure 2). Below 250 km, however, there are other slow features, not directly associated with surface tectonics, which predominate, in particular in the center of the Pacific Ocean.

Even though the tomographic models result from a formal inversion, damping and incomplete knowledge of data and model uncertainties make it difficult to assess the true resolution of our models. For example, a question which might be asked is whether the deep extent of fast velocities beneath West Africa is well resolved and imaged. If it is, the velocity structure beneath this shield is different from that seen beneath the Canadian shield (Grand and Helmberger, 1984), where faster than average velocities appear to terminate at 200–250 km depth.

One test which can be made is to see how Canadian shield structure is imaged in S20U7L5. Figure 3 shows a comparison between the vertical velocity profile SNA (Grand and Helmberger, 1984), representative for the Canadian shield, and S20U7L5 evaluated at a point just South of Hudson Bay. The agreement between the two is striking, both in terms of the overall amplitude of the perturbation, and the depth at which heterogeneity becomes small. Note that the velocity jump at 220 km is in our starting model (PREM), and that the smooth perturbations appear to counteract it. Also, there is agreement between SNA and S20U7L5 on the vertical gradient below 400 km, which disagrees with PREM.

A similar comparison can be made between the model TNA (Grand and Helmberger, 1984), and S20U7L5 (Figure 3). The agreement is not as striking as for the shield structure, which may in part be due to the fact that TNA was derived from data which sampled a variety of tectonic environments, including the East Pacific Rise, in addition to western US.

While the lithospheric root beneath West Africa extends deeper than that beneath the Canadian shield, the velocity structure beneath several other stable continental interiors are very similar to each other, as well as to SNA. Figures 4 shows a composite of six different velocity profiles which show similarities, not only in the upper few hundred kilometers, but also in the deepest part of the upper mantle.

Remaining Issues

The model S20U7L5 predicts all the datasets that went into its derivation well, indicating that the observations are compatible and complementary. Three concerns remain to be addressed before we finalize the model:

- Are the corrections for shallow structure (crustal thickness, etc.) adequate? While linearized corrections are adequate for longer period data (see Woodhouse and Dziewonski, 1984), we will investigate the effects of using more exact crustal corrections for the intermediate period surface waves.

- Is the lower upper mantle (250–600 km) well resolved? We have recently developed a new dataset of very long-period surface waves which we will include in the inversion. This should provide better constraints on the structure in this depth range.

- Are we damping the structure too much in the lower mantle? We will incorporate the additional datasets of all major teleseismic arrivals which we have been measuring from waveform data over the last two years. Several of these phases have sensitivity

primarily in the lower mantle, and incorporation of them will improve the resolution there.

Conclusions and Recommendations

Intermediate period surface waves provide excellent global coverage and sampling of shallow upper mantle structure. The inclusion of dispersion data for these waves in the derivation of the new model S20U7L5 has resulted in a higher resolution and better constrained model of the shear wave velocity in the upper mantle. Several interesting features are seen in the new model, including striking similarities of structure beneath continental cratons. In West Africa, however, fast velocities appear to extend to 500 km depth, while beneath the Canadian shield the fast structure terminates at around 300 km. Ridges also show a great variability in their expression at depth, with the Indian and Antarctic ridges having a distinct expression down to at least 200 km depth.

Lateral variations in S velocity in the upper 200 km of the mantle (as imaged in S20U7L5) are large, -5% – +7%. It is likely that in order to resolve heterogeneities on shorter length-scales than those seen in S20U7L5, new tools have to be developed which take better account of wave propagation effects in heterogeneous media. In addition, improved corrections for crustal thickness and crustal structure will make it possible to better resolve mantle velocities just below the Moho. Incorporation of additional seismic data for regional distances (e.g. Pn, Sn) should also help to improve the resolution in the shallowest mantle.

By combining a large number of diverse seismological observations, we have made progress towards obtaining higher resolution tomographic images of the regional scale elastic structure globally and beneath Eurasia. Large and regional scale heterogeneity in the mantle has been shown to bias seismically derived event locations, and it appears likely that further improvements in locations can be achieved by correcting for better known elastic heterogeneity in the Earth's mantle.

References

Dziewonski, A. M., Mapping the lower mantle: Determination of lateral heterogeneity in P velocity up to degree and order 6, *J. Geophys. Res.*, **89**, 5929-5952, 1984.

Ekström, G., J. Tromp, and E. W. Larson, Measurements and models of global surface wave propagation (abstract), *EOS, Trans. Am. Geophys. Un.*, **74**, 438, 1993.

Grand, S. P., and D. V. Helmberger, Upper mantle shear structure of North America, *Geophys. J. R. Astron. Soc.*, **76**, 399–438, 1984.

Mooney, W. D., Global crustal structure, *EOS, Trans. Am. Geophys. Un.*, **75**, 57, 1994.

Su, W.-J., R. L. Woodward and A. M. Dziewonski, Degree-12 Model of Shear Velocity Heterogeneity in the Mantle, *J. Geophys. Res.*, **99**, 6945–6980, 1993.

Woodhouse, J. H., and A. M. Dziewonski, Mapping the upper mantle: three-dimensional modeling of Earth structure by inversion of seismic waveforms, *J. Geophys. Res.*, **89**, 5953-5986, 1984.
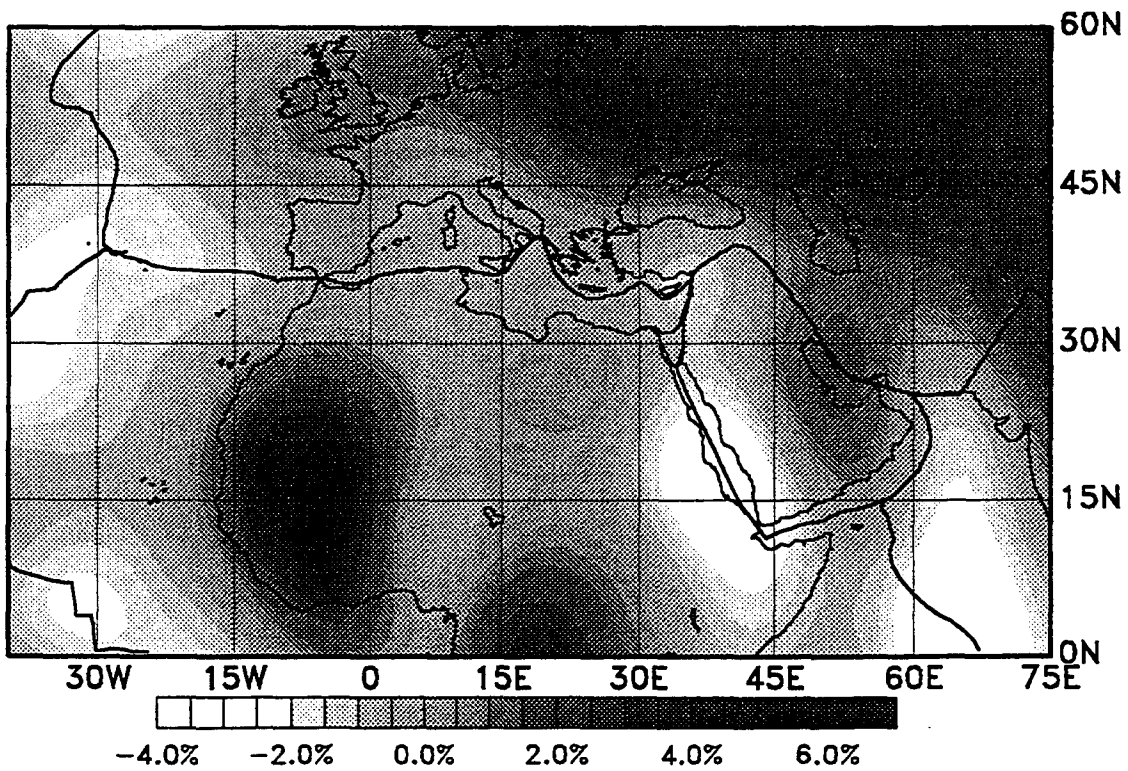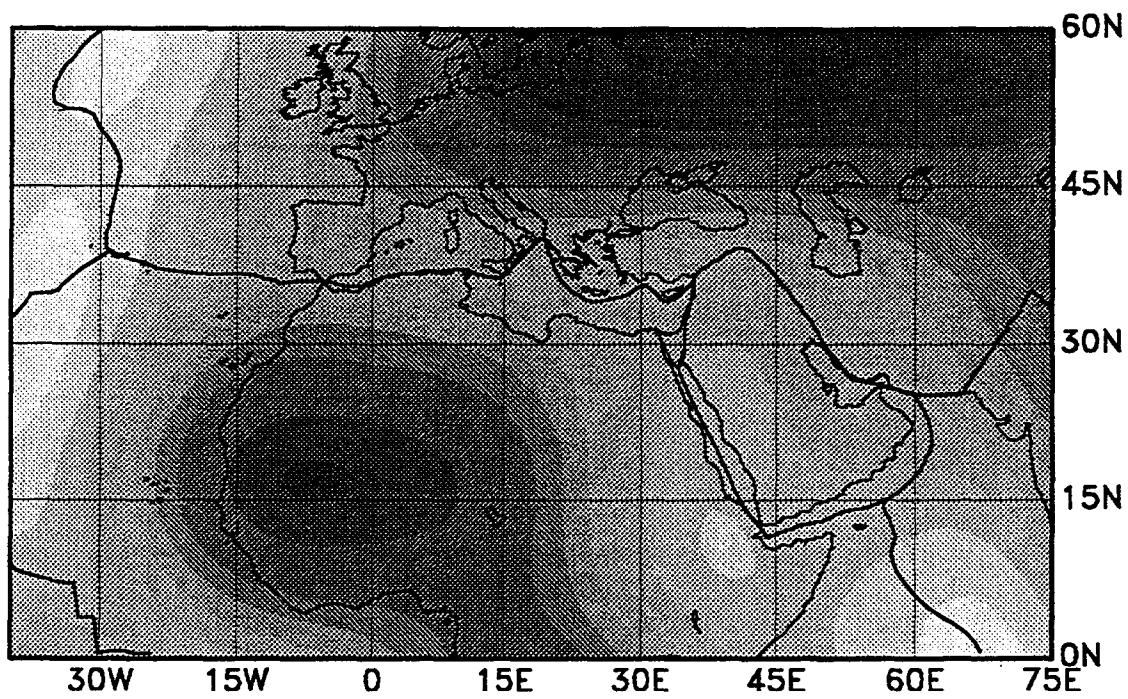
Figure 1 Top panel shows the velocity perturbations with respect to the global average at 150 km depth as seen in S12WM13 for the Mediterranean area. The bottom panel shows the same area, but for the model S20U7L5.
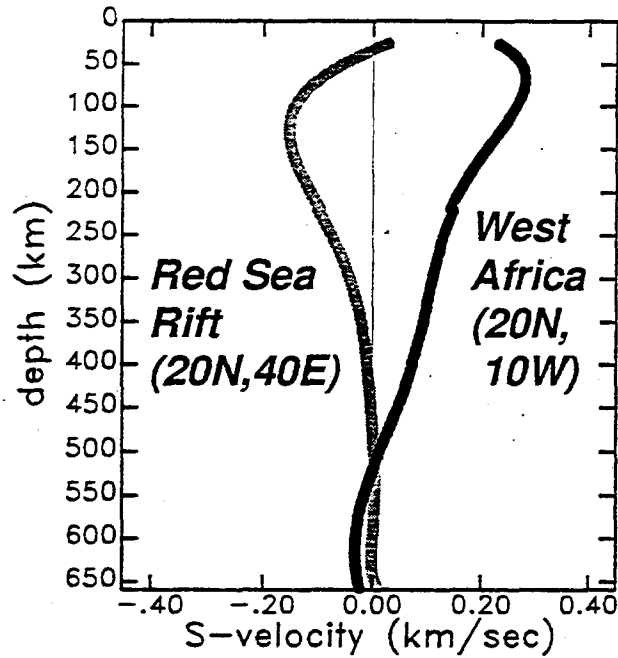
Figure 2 Vertical profiles of velocity perturbation with respect to the global average for two locations in Figure 1 associated with large velocity perturbations, West Africa and the Red Sea Rift. In the West African profile, fast velocities continue to 500 km depth, while the Red Sea Rift profile shows slow velocities down to 400 km depth.
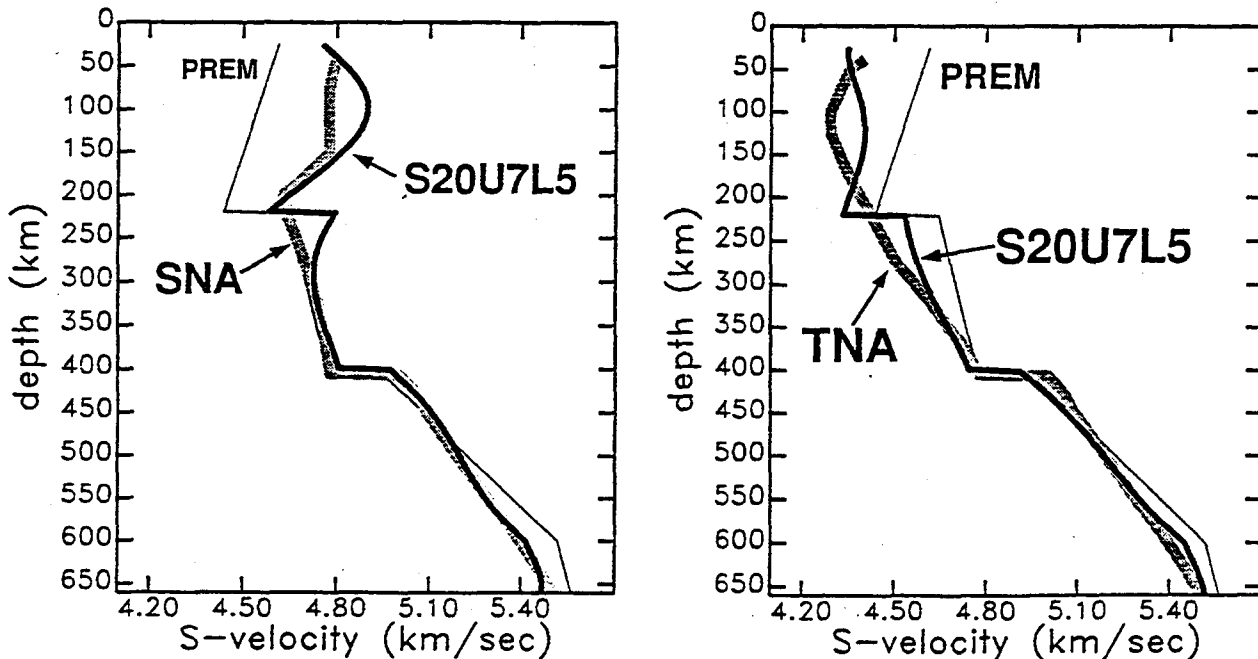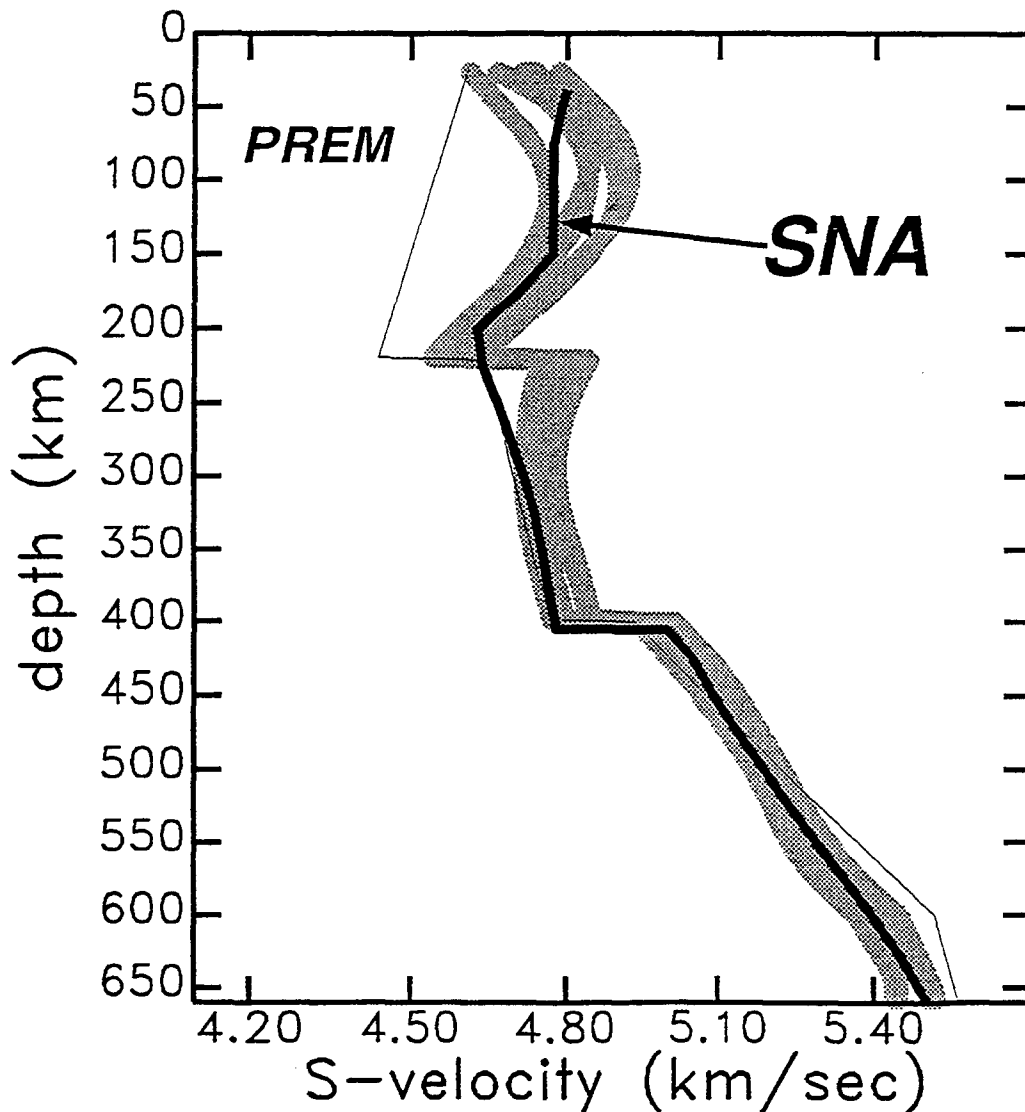

Figure 3 Vertical velocity profiles for two locations chosen to coincide with the regions analyzed by Grand and Helmberger (1984) in the development of the models SNA and TNA. Velocities for PREM, SNA, TNA, and S20U7L5 are shown with different line styles.

624

Figure 4 Vertical velocity profiles beneath six points located within stable continental interiors. Also shown, with the thick solid line, is the SNA structure. PREM is shown with the thin solid line.